

# Effect of an Intravitreal Antisense Oligonucleotide on Vision in Leber Congenital Amaurosis due to a Photoreceptor Cilium Defect

Artur V. Cideciyan<sup>1\*</sup>, Samuel G. Jacobson<sup>1\*</sup>, Arlene V. Drack<sup>2</sup>, Allen C. Ho<sup>3</sup>, Jason Charng<sup>1</sup>, Alexandra V. Garafalo<sup>1</sup>, Alejandro J. Roman<sup>1</sup>, Alexander Sumaroka<sup>1</sup>, Ian C. Han<sup>2</sup>, Maria D. Hochstedler<sup>2</sup>, Wanda L. Pfeifer<sup>2</sup>, Elliott H. Sohn<sup>2</sup>, Magali Taiel<sup>4</sup>, Michael R. Schwartz<sup>4</sup>, Patricia Biasutto<sup>4</sup>, Wilma de Wit<sup>4</sup>, Michael E. Cheetham<sup>5</sup>, Peter Adamson<sup>4,5</sup>, David M. Rodman<sup>4</sup>, Gerard Platenburg<sup>4</sup>, Maria D. Tome<sup>4</sup>, Irina Balikova<sup>6</sup>, Fanny Nerinckx<sup>6</sup>, Julie De Zaeytijd<sup>6</sup>, Caroline Van Cauwenbergh<sup>6</sup>, Bart P. Leroy<sup>6</sup>, Stephen R. Russell<sup>2</sup>

<sup>1</sup>Scheie Eye Institute, Department of Ophthalmology, Perelman School of Medicine, University of Pennsylvania, Philadelphia, PA, USA. <sup>2</sup>Department of Ophthalmology and Visual Sciences, Carver College of Medicine, University of Iowa, Iowa City, IA, USA. <sup>3</sup>Wills Eye Hospital, Thomas Jefferson University, Philadelphia, USA. <sup>4</sup>ProQR Therapeutics, Netherlands. <sup>5</sup>UCL Institute of Ophthalmology, London, UK. <sup>6</sup>Department of Ophthalmology, Ghent University and Ghent University Hospital, Ghent, Belgium.

\*Correspondence to:

Artur V. Cideciyan, Scheie Eye Institute, University of Pennsylvania, 51 N. 39th Street, Philadelphia, PA 19104, USA; Email: [cideciya@pennmedicine.upenn.edu](mailto:cideciya@pennmedicine.upenn.edu)

Samuel G. Jacobson, Scheie Eye Institute, University of Pennsylvania, 51 N. 39th Street, Philadelphia, PA 19104, USA; Email: [jacobsos@pennmedicine.upenn.edu](mailto:jacobsos@pennmedicine.upenn.edu)

33           **Photoreceptor ciliopathies constitute the most common molecular**  
34 **mechanism of the childhood blindness Leber congenital amaurosis (LCA). Ten**  
35 **LCA patients carrying the c.2991+1655A>G allele in the ciliopathy gene**  
36 ***CEP290* (Centrosomal protein 290) were treated (NCT03140969) with**  
37 **intravitreal injections of an antisense oligonucleotide to restore correct**  
38 **splicing. There were no serious adverse events and vision improved at 3**  
39 **months. The visual acuity of one exceptional responder improved from light**  
40 **perception to 20/400.**

41

42           Leber congenital amaurosis (LCA) is a childhood blindness with severe vision  
43 loss and progressive degeneration of rod and cone photoreceptors. The first  
44 breakthrough in therapy for LCA was in the form caused by bi-allelic *RPE65*  
45 mutations<sup>1</sup> where the primary defect is in retinal pigment epithelium (RPE) cells<sup>2</sup>. The  
46 more common molecular mechanisms of LCA involve a primary ciliopathy of rod and  
47 cone photoreceptors. A deep intronic allele (c.2991+1655A>G) is a frequent cause of  
48 LCA ciliopathies due to *CEP290* (Centrosomal protein 290) mutations<sup>3</sup>. This allele  
49 results in a classic splicing defect, creating a premature truncation codon  
50 p.(Cys998\*), likely subjecting the transcript to nonsense-mediated decay. Most  
51 patients lose all rod photoreceptors<sup>4</sup> but retain a central island of poorly functioning  
52 cone photoreceptors (Fig.1a) over many decades<sup>5</sup>, thereby creating an opportunity  
53 for therapy.

54           An antisense oligonucleotide (AON) was designed to restore correct splicing  
55 in the retina<sup>6</sup> (Fig.1b), and we are assessing its safety and tolerability in a clinical trial  
56 involving intravitreal injections (ClinicalTrials.gov number: NCT03140969).

57 Substantial improvement in vision in one patient prompted the decision to perform  
58 interim analyses of all data. Ten subjects were injected at least once and up to four  
59 times (Extended Data Table 1, Supplementary Table 1); eight subjects had at least 3  
60 months and four subjects had at least 6 months of follow up after the first injection.  
61 There were no severe adverse events and no events met stopping criteria. There  
62 was no intraocular inflammation: ocular treatment emergent adverse events were  
63 mild to none (Supplementary Information and Supplementary Tables 2 and 3). There  
64 were no retinal changes apparent during the three months after the first injection on  
65 cross-sectional (Extended Data Fig.1) or en face imaging (Extended Data Fig. 2).

66 Visual acuity is a standard method to evaluate efficacy. Baseline visual  
67 acuities ranged from 1.1  $\log_{10}$  MAR to light perception (LP) in study eyes, and 0.7  
68  $\log_{10}$  MAR to LP in untreated contralateral eyes (Extended Data Table 1). After one  
69 month, there were no changes in visual acuity; at three months, one patient had a  
70 large (2.7  $\log_{10}$  MAR) improvement and four other patients had smaller  
71 improvements from baseline that were equal or greater than the 0.3  $\log_{10}$  MAR  
72 commonly considered as clinically meaningful (Fig.1d). Interocular comparison at  
73 baseline showed treated eyes to be 0.12  $\log_{10}$  MAR (6 letters) worse than untreated  
74 eyes; by three months after intervention, however, interocular asymmetry reversed  
75 and treated eyes were 0.54  $\log_{10}$  MAR (26 letters) better than untreated eyes  
76 (Extended Data Fig.3c). Statistical analysis showed a significant effect at three  
77 months after treatment. At three months, subjects received a second injection  
78 (Extended Data Table 1). Six subjects had data to months 4 and 5 and four subjects  
79 to month 6. Improvements over baseline were retained at six months (Extended Data  
80 Fig.3).

81 LCA patients tend to show oculomotor instability ranging from fine nystagmus  
82 to large amplitude 'wandering' eye movements<sup>5</sup>. Consistent with some clinical  
83 observations, imaging of the eyes at three months showed a tendency towards  
84 improved ocular stability of treated eyes when presented with a fixation light but not  
85 when in a darkened room without fixation (Extended Data Fig.4). The average  
86 improvement was 0.13 log mm at three months and grew to 0.27 log mm at six  
87 months. The six month time point showed a significant effect.

88 To better quantify changes in photoreceptor function due to intervention, the  
89 intensity of dimmest lights detected in the dark were evaluated with full-field stimulus  
90 testing (FST). Before intervention, 7 of 8 patients demonstrated light thresholds  
91 ranging from -2.2 to 3.3 log<sub>10</sub> cd.m<sup>-2</sup> for red, and -2.5 to 2.3 log<sub>10</sub> cd.m<sup>-2</sup> for blue  
92 flashes (Extended Data Fig.5). Chromatic differences were consistent with detection  
93 by cone photoreceptors at baseline in all patients but P7 who had function mediated  
94 by rod photoreceptors. By two and three months, both red and blue thresholds  
95 showed improvements in many treated eyes (Fig.1e,f). At baseline, there was  
96 symmetry between the eyes with interocular differences averaging less than 0.02  
97 log<sub>10</sub>. After the injections, an interocular asymmetry developed by three months  
98 favoring better thresholds in treated eyes (-0.37±0.72 log<sub>10</sub> for red, -0.82±0.83 log<sub>10</sub>  
99 for blue, respectively; Extended Data Fig.5e,f). Statistical analysis showed a  
100 significant effect at months 1, 2, 3 and 6 (Extended Data Fig.5).

101 CEP290 ciliopathy is well known to affect the anatomy of photoreceptors<sup>4,5</sup>.  
102 Changes to photoreceptor ciliary anatomy were studied with cross-sectional images  
103 from a subset of patients with analyzable data at the fovea (Extended Data Fig.6). P2  
104 had foveal atrophy and evidence on microperimetry for fixation located in the

105 temporal parafovea of the treated eye. P4 and P7 showed an apparent increase in  
106 the reflection originating near the junction between the inner and outer segments  
107 (Extended Data Fig.6c) and P7 showed lengthening of inner and outer segments  
108 (Extended Data Fig.6e). Such findings were not seen in the untreated eyes  
109 (Extended Data Fig.6b,d,f).

110 Functional vision was assayed with a multi-luminance mobility course. Mobility  
111 scores showed a tendency for improvement at two and three months but changes  
112 were mostly symmetric between the eyes and there was no significant effect  
113 (Extended Data Fig.7).

114 Patient P2 was an exceptional responder who first reported substantial visual  
115 improvements 6 weeks after treatment. These findings led to a series of additional  
116 research studies. One year previously, P2 had visual acuities of LP in both eyes. At  
117 baseline, vision in both eyes remained LP (Fig.2a). The standard ETDRS letter  
118 acuity chart at 1m, and all the Berkeley Rudimentary Vision Test cards at 1 and 0.25  
119 m were not seen by either eye. At 1 month after the 160  $\mu$ g dose, visual acuities  
120 remained at LP (Fig.2a). At 6 weeks, the patient self-reported that, for the first time in  
121 decades, lights were seen with increasing clarity and brightness, but only in the  
122 treated eye.

123 At month 2, the patient could read the first three lines of the standard ETDRS  
124 chart at 1 m with the treated eye (corresponding to a visual acuity of 1.46  $\log_{10}$  MAR  
125 or Snellen equivalent of 20/580) but could not distinguish any letters with the  
126 untreated eye which remained LP (Fig.2a). Over the next 4 months, including an  
127 intervening maintenance dose of 80  $\mu$ g after the 3-month visit, there was incremental  
128 increase in acuity to 1.28  $\log_{10}$  MAR (Fig.2a). To better localize the retinal origin of

129 the improved acuity, we used a modified microperimeter and stimulated the macula  
130 directly. With the treated eye at the 2-month visit, the patient was able to distinguish  
131 orientation of achromatic gratings at  $1.37 \log_{10}$  MAR similar to the standard ETDRS  
132 results supporting a macular origin for improved acuity (Fig.2a). Chromatic gratings  
133 were used to distinguish between photoreceptor types mediating acuity. With red  
134 stimuli, the patient was able to distinguish orientation of gratings at  $1.50 \log_{10}$  MAR,  
135 whereas with blue stimuli he could only see gratings at  $1.97 \log_{10}$  MAR (Fig.2b).  
136 Between 3 and 6 months, chromatic acuities improved further (Fig.2b).

137 We used FST to evaluate detection of chromatic stimuli pre- and post-  
138 treatment in each eye under dark- and light-adapted conditions (Fig.2c-f). Results  
139 indicated mediation by cone photoreceptors under both conditions at all visits, and in  
140 both eyes. Thresholds remained without change from baseline in the untreated eye,  
141 for all visits, all stimuli and under different adaptation conditions. In the treated eye,  
142 however, there was an improvement in thresholds post-treatment compared to  
143 baseline. Threshold changes at 6 months were  $0.71$  and  $0.55 \log_{10}$  units for red  
144 FSTs under dark- and light-adapted conditions, respectively, and  $1.21$  and  $0.77 \log_{10}$   
145 units for blue FSTs under dark- and light-adapted conditions, respectively. Statistical  
146 analysis showed a significant effect at all post-treatment visits for dark-adapted  
147 conditions (Fig.2c,d) and all visits except for month 1 for light-adapted conditions  
148 (Fig.2e,f). Importantly, the large improvements of P2 were not the sole driver of the  
149 significance of the clinical trial cohort. Removing P2 from the analyses did not  
150 change the main statistical conclusion supporting significant improvements of visual  
151 acuity and FST at 3 months (Extended Data Table 2).

152 Advancing from an era of identifying causative genes in LCA, we are now  
153 using this information to design molecular-based therapies for these otherwise  
154 incurable forms of blindness. We now report that a primary photoreceptor ciliopathy  
155 can show improvement in vision using an AON therapy targeting pre-mRNA splicing.  
156 The improvement is noticeable to the patients and quantifiable with a number of  
157 outcome measures. Many questions remain as to the longevity of the efficacy and  
158 the value and safety of further dosage, but this evidence of positive visual change is  
159 a large translational step to the clinic for a childhood blindness with a wide window of  
160 therapeutic opportunity<sup>5</sup>.

161

## 162 **Methods**

163 Methods, including statements of data availability and any associated accession  
164 codes and references, are available online.

165

## 166 **Acknowledgements**

167 This work was supported by clinical trial contracts from ProQR Therapeutics to site  
168 principal investigators (PIs), A.V.C., B.P.L., and S.R.R..

169

## 170 **Author contributions**

171 A.V.C. and S.G.J. contributed to the clinical study design and protocol development,  
172 performed clinical investigation of patients, reviewed, analyzed and interpreted the  
173 data and wrote the draft manuscript and its revisions; M.T., M.R.S., P.B., W.dW.,  
174 P.A, D.M.R., G.P., and M.D.T. developed the clinical study protocol, reviewed the  
175 data and contributed to all drafts of the manuscript; A.V.D., B.P.L., and S.R.R.  
176 performed the clinical investigation of patients and contributed to the clinical study  
177 design and protocol development, and contributed to all drafts of the manuscript;  
178 A.C.H., F.N., and S.R.R. performed the injections; J.C., A.V.G., A.J.R., A.S., I.C.H.,  
179 M.D.H., W.P., E.H.S., I.B., and C.V.C. supported clinical investigation of the patients;

180 A.J.R. performed the statistical analyses; P.B., P.A. and M.E.C. performed in vitro  
181 experiments determining clinical dosing strategy.

182

183 **Competing interests**

184 M.T., M.R.S., P.B., W.dW., P.A., D.M.R., G.P., and M.D.T. are employees and stock  
185 holders of ProQR Therapeutics. M.E.C. was a consultant for ProQR Therapeutics.

186

187 **References**

- 188 1. Russell, S.R. et al. *Lancet*. **390**, 849-860 (2017).
- 189 2. Jacobson, S.G., et al. *Proc Natl Acad Sci USA*. **102**, 6177-82 (2005).
- 190 3. den Hollander et al., *Am J Hum Genet*. **79**, 556-61 (2006).
- 191 4. Cideciyan, A.V., et al. *Hum Mol Genet*. **20**, 1411-23 (2011).
- 192 5. Jacobson, S.G., et al. *Invest Ophthalmol Vis Sci*. **58**, 2609-2622 (2017).
- 193 6. Dulla, K., et al., *Mol Ther Nucleic Acids*. **12**, 730-40 (2018)

194

195

196

197 **Figure Legends**

198 **Fig. 1 | Photoreceptor ciliopathy caused by c.2991+1655A>G allele in the**  
199 **CEP290 gene and its treatment with antisense oligonucleotide QR-110 injected**

200 **intravitreally. a**, Boundaries of the retained central elliptical islands in 20 patients  
201 with this allele. **b**, Schematic for the mechanism of action of QR-110. Without  
202 treatment (left), the mutation creates a strong splice donor site, and aberrant splicing  
203 results in the insertion of a cryptic Exon X in many *CEP290* mRNA transcripts. Exon  
204 X contains a premature stop codon, predicted to result in an inactive, truncated  
205 CEP290 protein, and/or to target the mutant mRNA transcript for nonsense mediated  
206 decay, significantly lowering the levels of wild-type CEP290 protein. With treatment  
207 (right) QR-110 binds to the pre-mRNA and blocks aberrant splicing, thereby skipping  
208 Exon X in mRNA, resulting in increased levels of wild-type transcripts and CEP290  
209 protein. **c**, Injection into the vitreous humor. **d-f**, Change in  $\log_{10}$  units from baseline  
210 of visual acuity and full-field stimulus testing (FST) using red and blue flashes  
211 presented in the dark. All three measures of visual function show significant  
212 improvements in treated eyes at 3 months. Larger symbols are averages from 10  
213 patients at BL and M1, and 8 patients at M2 and M3. Smaller symbols are individual  
214 data points. Error bars= $\pm 1$  sd, BL=average of two pre-treatment baselines, M1-  
215 M3=post-treatment evaluations at months 1-3 after the administration of an  
216 intravitreal dose of 160 or 320  $\mu\text{g}$  after BL. Linear mixed-effects models were used  
217 for the statistical analysis.

218

219

220 **Fig. 2 | Six month evaluation of patient P2 who had an exceptional**  
221 **improvement in visual function. a**, Visual acuity (in  $\log_{10}$  MAR, minimum angle of  
222 resolution) showing large and sustained improvement in the treated eye starting at  
223 month 2 (M2) and continuing at least to month 6. Testing performed with achromatic  
224 letters and gratings under free-viewing conditions (filled symbols) or achromatic  
225 gratings projected onto the macula (open symbols). LP=light perception; NS=not  
226 seen. **b**, Acuity with chromatic (Red or Blue) gratings projected onto the macula  
227 starting at M2 and continuing to M6. The results suggest long- and middle-  
228 wavelength sensitive cone photoreceptors are the dominant contributors to acuity. **c-**  
229 **f**, FST threshold change from baseline using red and blue flashes presented under  
230 dark-adapted (DA) and light adapted (LA,  $10 \text{ cd.m}^{-2}$  white) conditions. Symbols are  
231 averages from repeated measures obtained at each visit (for most visits  $n=12$ ,  
232 except for BL DA where  $n=30-34$ , M3 DA where  $n=18$ , and some visits where  $n=10-$   
233  $16$ ), error bars= $\pm 1$  sd, BL=average of two pre-treatment baselines, M1-M6=post-  
234 treatment evaluations at months 1 through 6. Linear mixed-effects models were used  
235 for the statistical analysis. Patient was administered a single intravitreal dose of  $160$   
236  $\mu\text{g}$  after the BL visit, and a further maintenance dose of  $80 \mu\text{g}$  after the M3 visit.

237

238

239

240

241

242

243

244 **Methods**

245 **Study medication and trial design.** QR-110 is a 17-mer RNA antisense  
246 oligonucleotide (AON) consisting of the following 5' to 3' sequence  
247 GGUGGAUCACGAGUUCA prepared as the sodium salt ( $C_{180}H_{219}N_{67}Na_{16}O_{101}P_{16}S_{16}$   
248 and molecular mass of 6313.51 Daltons). QR-110 drug substance was manufactured  
249 with all RNA bases 2'-O-methylribose modified with all inter-nucleotide linkages  
250 comprising phosphorothioate (BioSpring GmbH, Frankfurt, Germany). QR-110 was  
251 synthesized as GMP grade by solid state synthesis in the direction 3' to 5' and  
252 further purified by ion-exchange chromatography. Drug product was prepared by  
253 dissolving QR-110 drug substance (10mg/ml) in formulated phosphate buffered  
254 saline in depyrogenated vials and sterilized stoppers, and filter sterilized using 0.22  
255  $\mu$ m double filtration (Pyramid Laboratories, Inc., Costa Mesa, CA, USA).

256 QR-110 was designed to bind to a sequence within the exonic splicing  
257 enhancer sequence at intron 26 of the *CEP290* pre-mRNA<sup>6</sup>. The hybridization of the  
258 QR-110 is thought to modulate the RNA splicing process, blocking access to the  
259 active cryptic splicing site, and restoring preference for the wildtype splicing sites. A  
260 resulting increase of wildtype mRNA transcript leads to an increase of functional  
261 CEP290 protein<sup>6</sup>.

262 An open-label, multiple arm, multiple dose, dose escalation study was  
263 designed to evaluate the safety and tolerability of QR-110 administered via unilateral  
264 intravitreal (IVT) injection (to the worse eye) every three months for up to 1 year  
265 (ClinicalTrials.gov no. NCT03140969). The study is being conducted according to the  
266 Declaration of Helsinki as well as according to the principles of Good Clinical  
267 Practice. There are three sites (Iowa City, US; Philadelphia, US; and, Ghent,

268 Belgium) and Institutional Review Boards of the University of Pennsylvania, Wills  
269 Eye Hospital, University of Iowa and Ghent University approved the studies which  
270 complied with all relevant ethical regulations. Eligible subjects include males and  
271 females 6 years of age or older at screening with a clinical diagnosis of LCA and a  
272 molecular diagnosis of homozygosity or compound heterozygosity for the CEP290  
273 p.(Cys998\*) mutation. Of note, inclusion criteria for best-corrected visual acuity  
274 (BCVA) are better than or equal to light perception (LP) in both eyes, and equal to or  
275 worse than  $+0.6 \log_{10}$  of Minimum Angle of Resolution (MAR) (20/80 Snellen  
276 equivalent) in the worse eye and equal to or worse than  $+0.4 \log_{10}$  MAR (20/50  
277 Snellen equivalent) in the contralateral eye. Eligible, enrolled subjects receive up to 4  
278 administrations of QR-110 at 3-month intervals over the course of one year.

279

280 **Demographics and baseline characteristics of patients treated.** The date for  
281 study start (first visit of first patient) was October 16, 2017. The current report  
282 represents an interim analysis of the ongoing study as of the cutoff date of August  
283 15, 2018. Included are all ten subjects who have received one or more injections of  
284 QR-110 (Extended Data Table 1). Written informed consent (or informed assent and  
285 parental consent for pediatric subjects) was provided by each subject before the  
286 initiation of study activities. Ophthalmic and systemic safety aspects of the study  
287 were and continue to be monitored by an independent Data Monitoring Committee.  
288 There were 6 adult patients between the ages of 19 to 44 years, and 4 pediatric  
289 patients between 8 and 16 years. There were 5 males and 5 females. All subjects  
290 were compound heterozygotes for the c.2991+1655A>G p.(Cys998\*) allele and an  
291 additional mutant allele in the *CEP290* gene. Two patients were siblings, and two

292 patients carried the same mutations but were not known to be related. Subjects were  
293 assigned to receive one of two dose levels of QR-110. Three adult and two pediatric  
294 patients were assigned to a loading dose of 160 µg and a maintenance dose of 80  
295 µg QR-110. Three adult patients and two pediatric patients were assigned to a dose  
296 consisting of 320/160 µg QR-110 (Extended Data Table 1, Supplementary Table 1).

297

298 **Safety evaluations.** Ocular safety was assessed with standard eye examinations,  
299 including gradings of the anterior and posterior segment according to the  
300 Standardization of Uveitis Nomenclature<sup>7</sup>, and of the lens according to the Age-  
301 Related Eye Diseases Study Clinical Lens Grading System<sup>8</sup>. Near-infrared excited  
302 autofluorescence imaging, when possible, was used to document any changes in  
303 RPE pigmentation<sup>9</sup>. Systemic safety was evaluated with physical examinations at  
304 baseline and postoperative visits. Routine hematology; testing of serum chemistry,  
305 prothrombin time (with international normalized ratio), and partial thromboplastin  
306 time; and urinalysis were performed at baseline and postoperatively.

307

308 **Visual acuity.** Visual acuity (VA) was measured using Early Treatment Diabetic  
309 Retinopathy Study (ETDRS) methodology<sup>10</sup> at two baseline visits and post-injection  
310 visits starting at month 1. Best-corrected VA was scored as the number of letters  
311 correctly read after adjusting for distance (4m or 1m) and expressed as log<sub>10</sub> MAR to  
312 measure the range of acuities from 20/10 to 20/800 (or from -0.30 to +1.6 log<sub>10</sub>  
313 MAR). For patients not able to correctly read ETDRS letters at 1m, Berkeley  
314 Rudimentary Vision Test battery was performed<sup>11</sup> at distances of 1 m and 0.25 m to  
315 measure the range of acuities from 20/500 to 20/16,000 (or from +1.4 to +2.9 log<sub>10</sub>

316 MAR). Hand-motions (HM) acuity was assigned  $+3.0 \log_{10}$  MAR and light-perception  
317 (LP) was assigned  $+4.0 \log_{10}$  MAR.

318

319 **Imaging.** Spectral-domain Optical Coherence Tomography (OCT) was used to  
320 obtain cross-sectional imaging of the retina<sup>4,5</sup> (RTVue-100; Optovue, Fremont, CA, or  
321 Spectralis, Heidelberg Engineering, Heidelberg, Germany). All OCT images were  
322 aligned by straightening the major RPE reflection. In a subset of 4 patients, with  
323 reliable foveal scans available in both eyes at BL, month 1 and month 3 time points,  
324 quantitative analyses of the photoreceptor cilial anatomy was performed using  
325 longitudinal reflectivity profiles. Inner segment (IS) length was estimated between  
326 the outer limiting membrane peak and the peak originating near the junction of inner  
327 and outer segments (IS/OS). The outer segment length was estimated between the  
328 IS/OS peak and peak originating near the interface of OS tips and apical RPE  
329 processes. En face imaging with near-infrared illumination was performed with  
330 autofluorescence mode or reflectance mode using a confocal scanning laser  
331 ophthalmoscope<sup>4,5,9</sup> (HRA2 or Spectralis, Heidelberg Engineering, Heidelberg,  
332 Germany).

333

334 **Oculomotor Control and Instability (OCI).** To account for the wide spectrum of  
335 oculomotor abnormalities encountered in *CEP290*-LCA patients, an infrared video  
336 oculography method was used<sup>5</sup>. Two recordings were performed in a darkened  
337 room. One with a bright fixation light available along the primary gaze, and another  
338 without a fixation light.

339

340 **Full-field Stimulus Testing (FST).** Sensitivity to chromatic light flashes presented in  
341 the dark in dark-adapted eyes was measured with full-field stimulus testing (FST)  
342 developed specifically for patients with severe vision loss and oculomotor  
343 instability<sup>12</sup>. FST was tested with a commercial software<sup>13,14</sup>. For each color, eye,  
344 and visit, approximately 12 independent thresholds were obtained thus providing an  
345 estimate of intra-session variability. Large variability in FST usually indicates  
346 unreliable performance within a session. Exploratory analyses showed that 11  
347 sessions (out of 197) were associated with unusually large intra-session variances  
348 compared to previously published estimates of variability<sup>12</sup>. These sessions had  
349 intra-session standard deviation of  $>1.01 \log_{10}$  and were also classified as suspected  
350 outliers by Tukey's criteria (1.5xIQR above the third quartile). Statistical analyses  
351 were performed twice: one with the full data set and a second time excluding the 11  
352 sessions. Both analyses, with and without exclusions, supported the same statistical  
353 conclusions regarding a significant treatment effect from month 1 to 6; however,  
354 exclusion allowed presentation of the most conservative, internally consistent and  
355 repeatable data. Of additional note, at the three month time point, it was found out  
356 that one patient (P7) was mistakenly tested with a 'flash' stimulus (duration  $<4$  ms)  
357 instead of the 'pulse' stimulus (duration=200 ms) specified in the protocol. At the  
358 three month time point, the patient was tested with both types of stimuli to obtain a  
359 comparison.

360

361 **Mobility.** The visual navigation challenge (ORA-VNC<sup>TM</sup>) was used to assess mobility  
362 performance of patients at multiple levels of luminance<sup>15</sup>. There were four difficulty  
363 levels of the courses, and each course had several lighting conditions defining 20

364 'levels'. For each level there were several combinations of random obstacle  
365 placements that were used to avoid learning effects. A level of 0 represented failing  
366 to pass successfully any of the courses at any light level; and a level of 19  
367 corresponded to passing the most difficult course under dimmest light conditions. For  
368 each eye and each visit, the highest level course passed was recorded. Results from  
369 P7 were censored because of the unavailability of levels 13-19 at the time of both  
370 baseline visits. In addition, one of the baseline visits and the month 1 visit of P5 was  
371 censored for the same reason.

372

373 **Additional evaluations in the exceptionally responding patient.** Patient P2 was  
374 known to the investigators and previously evaluated with detailed non-invasive  
375 assessments of visual function and retinal structure<sup>4,5</sup>. Contemporaneous with the  
376 clinical trial, the patient was enrolled in additional research studies that had been  
377 approved by the University of Pennsylvania Institutional Review Board. The studies  
378 included FST under dark- and light-adapted conditions<sup>12,16</sup>. Specifically, the custom  
379 thresholding algorithm was based on a 4 dB/2 dB staircase with two response  
380 reversals (as opposed to the binary thresholding algorithm used by the  
381 manufacturer). In addition, there was a limited response-acceptance window to  
382 minimize the effect of extraneous responses not synchronized with the stimulus  
383 presentation. Both of these algorithmic features helped reduce variability especially  
384 in patients with severe vision loss. Spatial resolution was measured with achromatic  
385 and chromatic gratings<sup>17</sup>.

386

387 **Statistical analyses.** Linear mixed-effects models were used for the statistical  
388 analysis of all efficacy outcomes to account for the correlation structure and repeated  
389 measures within each data set. The baseline data were pooled from the two visits  
390 obtained before the first injection. Results from the two dose groups were pooled for  
391 statistical analyses. The models used an unstructured covariance matrix, restricted  
392 maximum likelihood estimation and the Satterhwaite's approximation for denominator  
393 degrees of freedom. Computations used the lme4 (ver. 1.1-17)<sup>18</sup> and lmerTest (ver.  
394 3.0-1)<sup>19</sup> packages from R statistical software (ver. 3.4.4, 2018-03-15)<sup>20</sup>.

395 For VA, the dependent variable was the minimum angle of resolution  
396 expressed in  $\log_{10}$  MAR. The model used Treatment-by-Visit interaction as fixed  
397 effects. Intercept and Visit were specified as random effects, with Patient as the  
398 grouping factor. The Treatment factor had two levels (treated and untreated eyes),  
399 and the Visit factor had seven levels (baseline and months 1, 2, 3, 4, 5 and 6). For  
400 OCI, the dependent variable was the variation of the radial distance of the center of  
401 pupil from the mean normal primary gaze locus over 30 s expressed in  $\log_{10}$  mm.  
402 The fixed effects and random effects were the same except Visit factor had three  
403 levels (baseline, month 3 and 6). Separate analyses were performed for OCI data  
404 recorded with and without fixation. For FST, the dependent variable was the visual  
405 threshold expressed in  $\log_{10}$  phot-cd.m<sup>2</sup>. The model used Treatment-by-Condition  
406 interactions as fixed effects in addition to Treatment-by-Visit. The Condition factor  
407 had two levels (blue and red). The random effects were the same as in the VA  
408 model. For mobility the dependent variable was the performance score, an ordinal  
409 variable ranging from 0 to 19. The same analysis was used for mobility as for VA by  
410 approximating the ordinal variable as a continuous variable. For Fig. 2, separate

411 analyses were performed for dark-adapted and light-adapted data. Analyses were  
412 identical to that of all other FST results except random effects were not specified as  
413 there was only a single patient.

414

415 **Reporting Summary.** Further information on experimental design is available in the  
416 Life Sciences Reporting Summary.

417

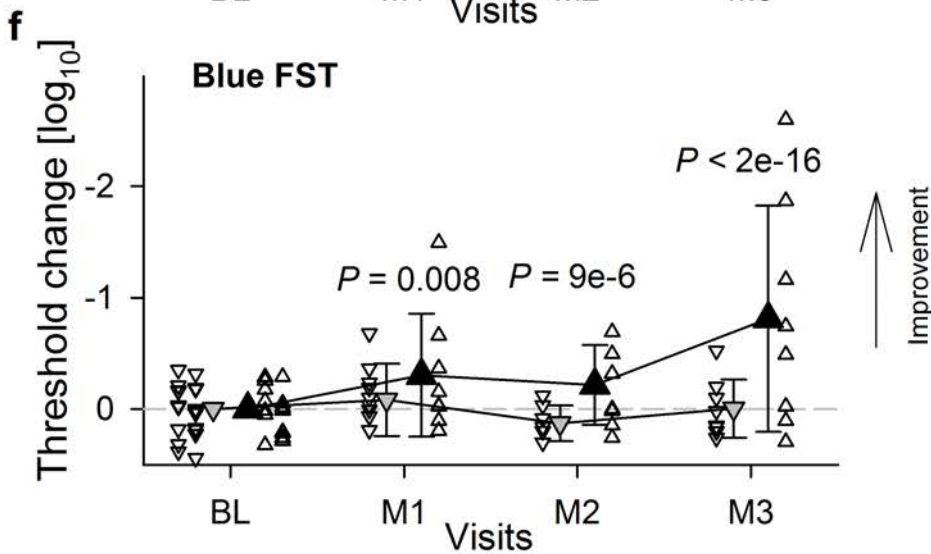
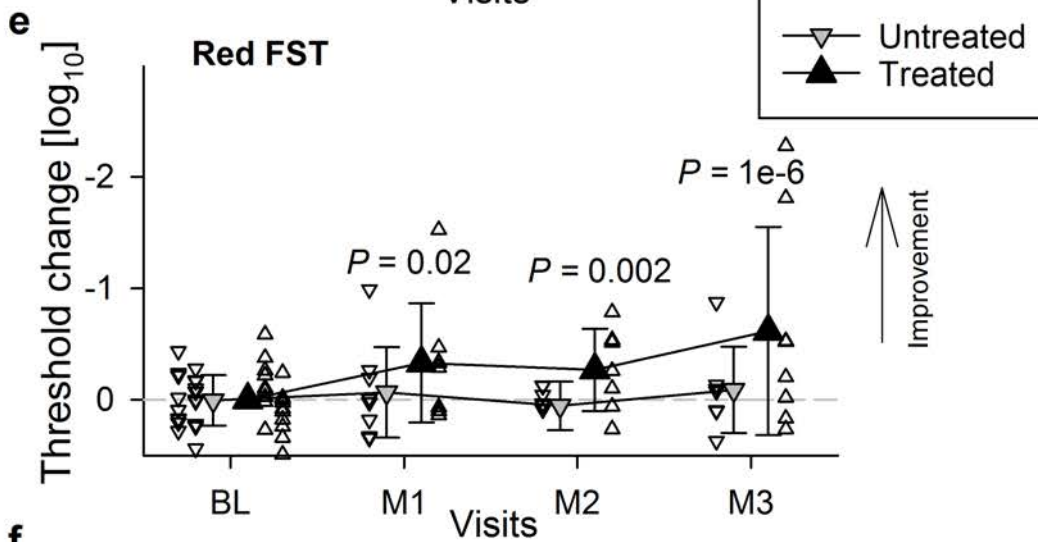
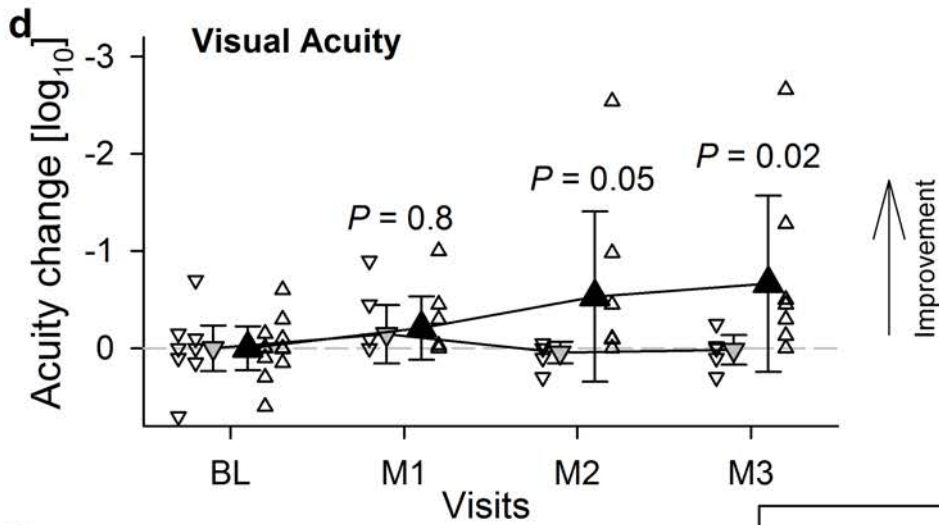
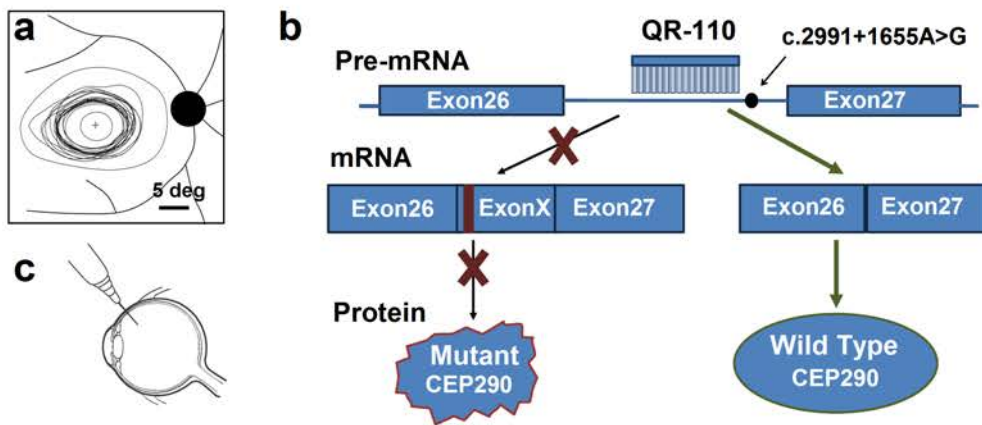
418 **Data availability.** All relevant patient-level data are displayed in Figures. All requests  
419 for data will be reviewed by ProQR Therapeutics and the Universities involved to  
420 verify if the request is subject to any intellectual property or confidentiality  
421 obligations. Patient-related data may be subject to confidentiality. Any data that can  
422 be shared will be released.

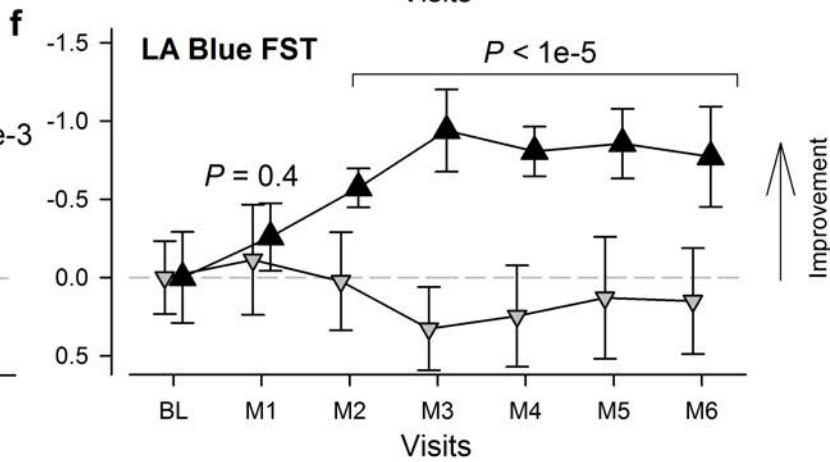
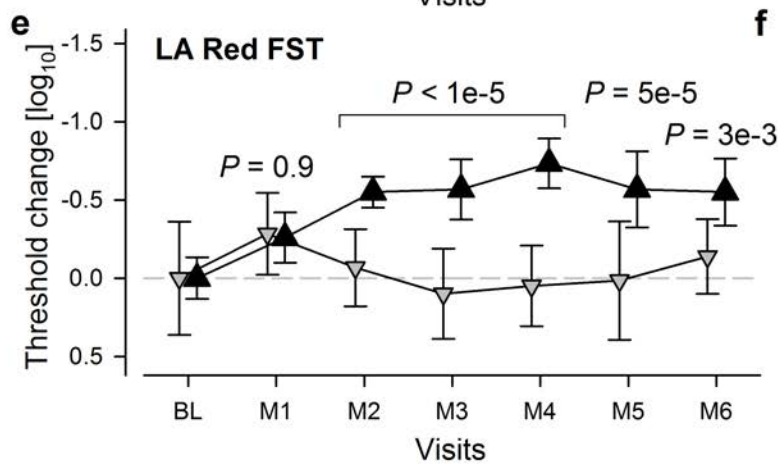
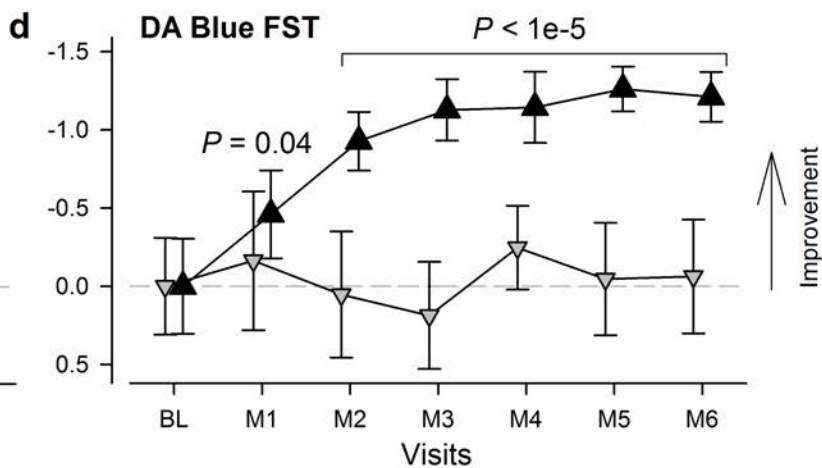
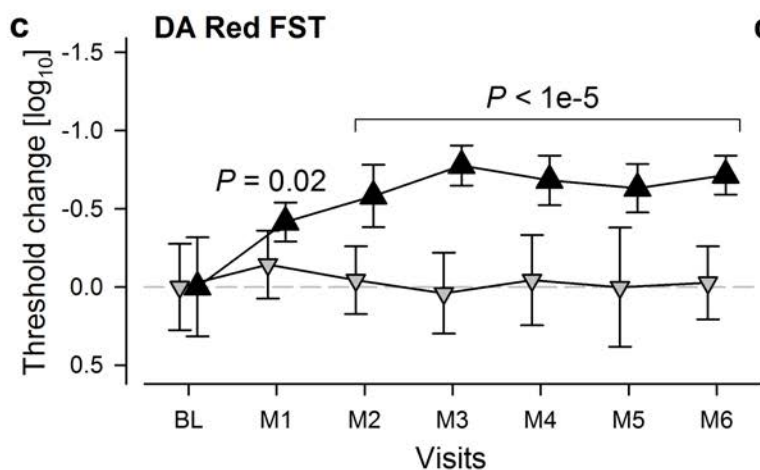
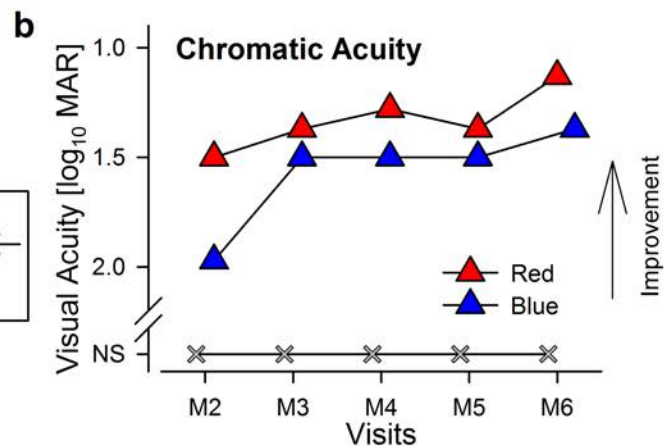
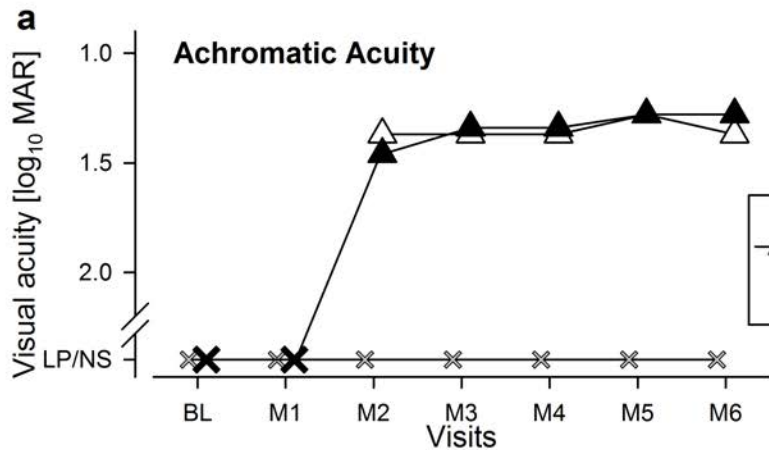
423

## 424 **References**

- 425 7. Jabs, D.A., et al., *Am J Ophthalmol.* **140**, 509-16 (2005).
- 426 8. Chew, E.Y., et al., *Ophthalmology.* **117**, 2112-9.e3 (2010).
- 427 9. Cideciyan, A.V., et al. *J Opt Soc Am A.* **24**, 1457-67 (2007).
- 428 10. Ferris, F.L., Kassoff, A., Bresnick, G.H., Bailey, I.L. *Am J Ophthalmol.* **94**, 91-96  
429 (1982).
- 430 11. Bailey, I.L., Jackson, A.J., Minto, H., Greer, R.B., Chu, M.A. *Optom Vis Sci.* **89**,  
431 1257-64 (2012).
- 432 12. Roman, A.J., Cideciyan, A.V., Aleman, T.S., & Jacobson, S.G. *Physiol Meas.* **28**,  
433 N51-6 (2007).
- 434 13. Klein, M., Birch DG. *Doc Ophthalmol.* **119**, 217-24 (2009).
- 435 14. Collison, F.T., Fishman, G.A., McAnany, J.J., Zernant, J., Allikmets, R. *Retina.*  
436 **34**, 1888-95 (2014).
- 437 15. Shapiro, A., et al. *Invest Ophthalmol Vis Sci.* **58**, E-Abstract 3290 (2017).
- 438 16. Jacobson, S.G., et al. *Hum Mol Genet.* **22**, 168-83 (2013).
- 439 17. Cideciyan, A.V., et al., *Invest Ophthalmol Vis Sci.* **57**, 3211-21 (2016)

- 440 18. Bates, D., Maechler, M., Bolker, B., Walker, S. *J Stat Softw.* **67**, 1-48 (2015).  
441 19. Kuznetsova, A., Brockhoff, P.B., Christensen, R.H.B. *J Stat Softw.* **82**, 1-26  
442 (2017).  
443 20. R Core Team <https://www.R-project.org/> (2018)  
444  
445  
446





## Extended Data Table 1: Baseline Participant Characteristics

Code	Sex	2 <sup>nd</sup> CEP290 Allele #	Age/Grp ~	Baseline VA [log MAR] +	Treated Eye @	Dose [ug] &	Num. of Inj. ^	Length of f/u [mon] \$
P1	M	c.2506_2507delGA	19 / A	LP / LP	RE	160 / 80	4	9.0
P2	M	c.4723A>T	41 / A	LP / LP	RE	160 / 80	3	7.0
P3	M	c.5668G>T	44 / A	2.3 / 2.4	LE	160 / 80	2	3.0
P4	F	c.4438-3delC	16 / P	2.5 / 2.5	RE	160 / 80	3	6.0
P5	M	c.6277delG	8 / P	1.9 / 2.1	LE	160 / 80	2	5.0
P6	F	c.3167_3168insA	21 / A	LP / LP	RE	320 / 160	3	6.5
P7	F	c.4723A>T	27 / A	1.1 / 0.7	RE	320 / 160	2	5.0
P9	F	c.4393C>T	24 / A	LP / LP	RE	320 / 160	1	1.0
P8	M	c.6277delG	10 / P	1.9 / 1.4	RE	320 / 160	2	3.0
P10	F	c.547_550delTACC	15 / P	LP / LP	RE	320 / 160	1	1.0

# all patients had c.2991+1655A>G/p.(Cys998\*) allele in common; nucleotide change and predicted effect of the additional allele shown

~ Age in years at the time of enrollment; A=adult; P=pediatric

+ Visual acuity in right / left eyes in logarithm of minimum angle of resolution (MAR); 0 log MAR corresponds to Snellen acuity of 20/20, 2 log MAR corresponds to 20/2000; LP=Light perception

@ RE=right eye, LE=left eye

& Loading / maintenance dose of QR110 injected intravitreally in a 50 uL volume

^ Intravitreal injections every 3 months

\$ Length of followup in months after the first injection

## Extended Data Table 2: Treatment effect at 3 months

		Mean change from BL* [ $\log_{10}$ ]	P-value +
<b>All patients (n=8)</b>			
VA	Treated eyes	<b>-0.67</b>	<b>0.022</b>
	Untreated eyes	0.02	
Red FST ~	Treated eyes	<b>-0.62</b>	<b>1E-06</b>
	Untreated eyes	-0.09	
Blue FST ~	Treated eyes	<b>-0.81</b>	<b>&lt; 2E-16</b>
	Untreated eyes	-0.01	
<b>Withholding data from P2 (n=7)</b>			
VA	Treated eyes	<b>-0.38</b>	<b>0.018</b>
	Untreated eyes	0.02	
Red FST ~	Treated eyes	<b>-0.63</b>	<b>3E-04</b>
	Untreated eyes	-0.16	
Blue FST ~	Treated eyes	<b>-0.76</b>	<b>2E-13</b>
	Untreated eyes	-0.04	

\* Negative values correspond to improvement of function compared to baseline (BL).

+ Linear mixed-effects models were used for the statistical analysis of all efficacy outcomes to account for the correlation structure and repeated measures within each data set. P-values for the significance of treatment-by-visit interactions

~ Sessions with an intravisit sd greater than 1.01 have been censored; conclusions are unchanged when censoring is not used

Treated

Untreated

BL

M1

M3

BL

M1

M3

P1

P2

P3

P4

P5

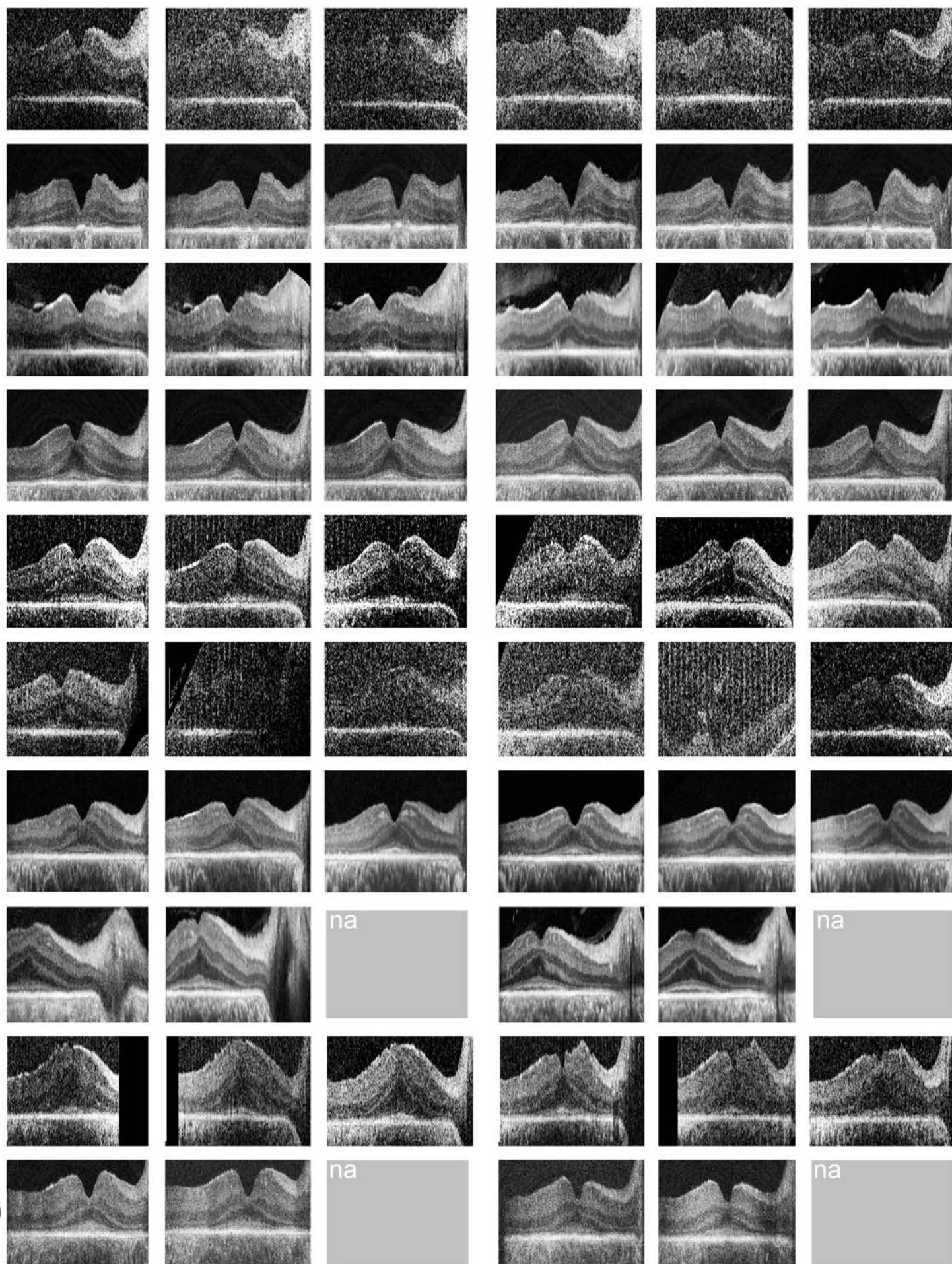
P6

P7

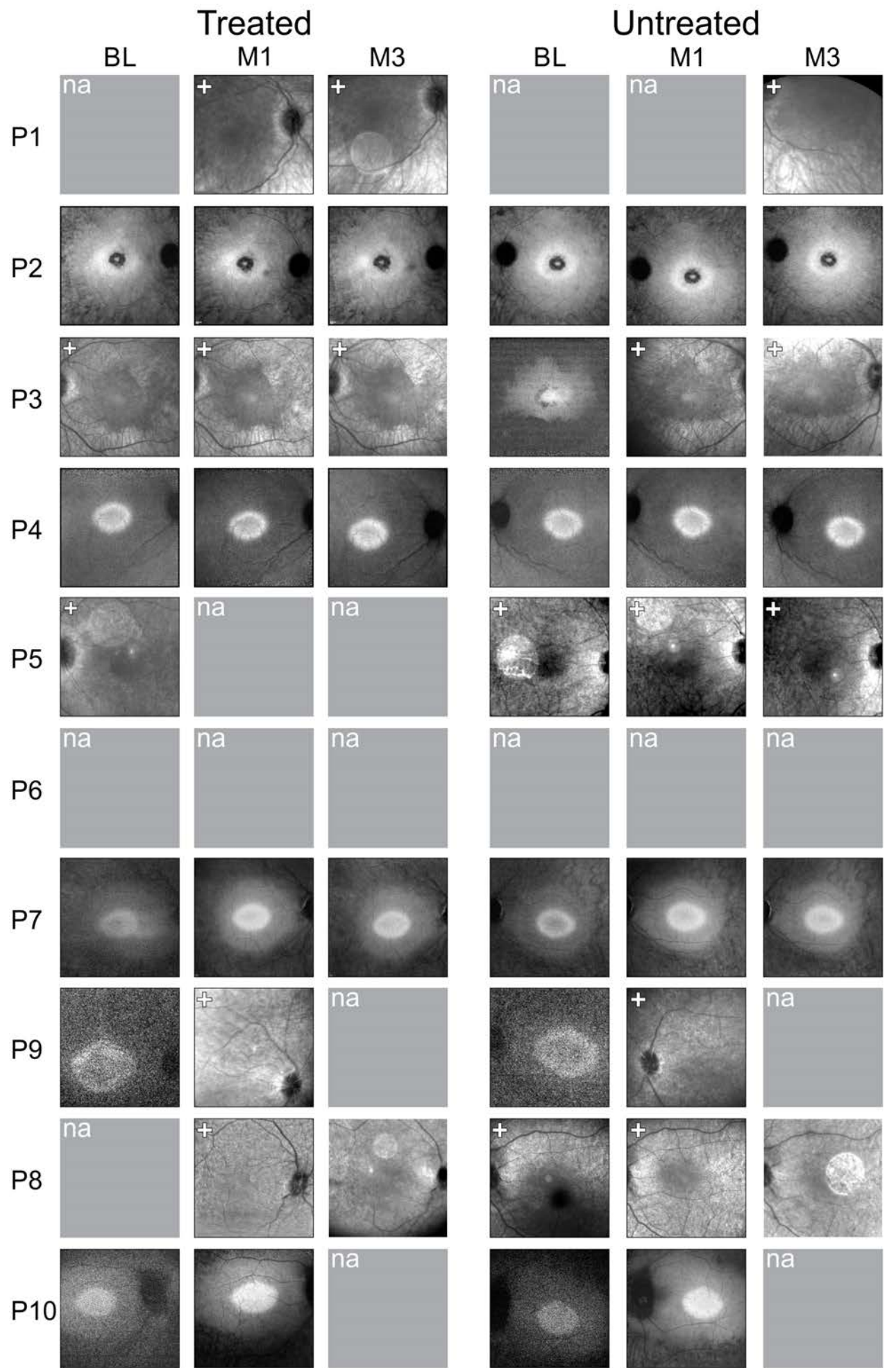
P9

P8

P10



100  $\mu\text{m}$   
1 deg



⊕ NIR-REF

10deg

